A Configurationally Stable Indenofluorene-Based Helical Diradicaloid

Álvaro Martínez-Pinel,[a] Luis Lezama,[b] Juan M. Cuerva,[a] Raquel Casares,[a] Víctor Blanco,[a] Carlos M. Cruz,[a]* Alba Millán[a]*

[a] Departamento de Química Orgánica and Unidad de Excelencia de Química aplicada a Biomedicina y Medioambiente, Facultad de Ciencias, Universidad de Granada, 18071 Granada, Spain;

[b] Departamento de Química Orgánica e Inorgánica, Facultad de Ciencia y Tecnología, Universidad del País Vasco, 48940 Leioa, Spain.

Supporting Information Placeholder

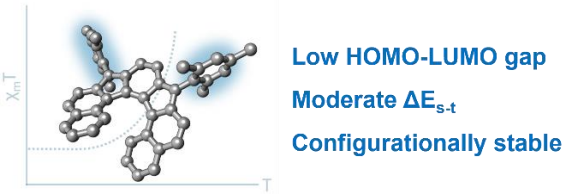

ABSTRACT: The synthesis and the optoelectronic, magnetic and chiroptical properties of a helically chiral diradicaloid have been reported. Dibenzoindeno[2,1-*c*]fluorene, the simplest configurationally stable chiral derivative of the family of the indenofluorenes, shows a low HOMO-LUMO gap and a moderate singlet-triplet gap. Enantiomers have been isolated and are configurationally stable. Electronic circular dichroism has been measured and dissymmetry factor calculated. Our experimental findings are supported by DFT calculations.

Indenofluorenes (IFs) are non-alternant conjugated hydrocarbons with alternating fused six- and five-membered rings.[1] The relative fusion pattern of the rings give access to a wide family of antiaromatic compounds (Figure 1) with attractive and varied properties.[2-13] Most of such properties are related with the diradical character provided by their pro-aromatic central quinodimethane unit.[14-15] Consequently, the IFs need to be stabilized thermodynamically or kinetically to tame the reactivity of the apical carbon of the five-membered rings (Figure 1, open-shell configurations).[16-17] The structural diversity and interesting properties of this class of compounds also invite to explore chirality.[18] The synergy of chirality and unpaired electrons has significant application in molecular optoelectronics and spintronics.[1,19-22] In this sense, substantial structural modifications have been carried out to provide chiral structure of IF derivatives.[23-26] Nevertheless, in these examples the basic 6-5-6-5-6 core of indenofluorene gets diluted and in some cases low racemization barriers preclude the isolation of enantiopure samples and thus the study of chiroptical properties. Remarkably, the simple indeno[2,1-*c*]fluorene (Figure 1) resembles the structure of a [5]helicene, but it is configurationally unstable.[4,5] π-Extension of the outermost rings would lead to explore novel helicenoids with enhanced configurational stability, maintaining the basic skeleton of IF. Additionally, the extension of the π-system together with the helical distortion should diminish the HOMO-LUMO and the singlet-triplet energy gaps,[27-30] making these molecules even more appealing for application.

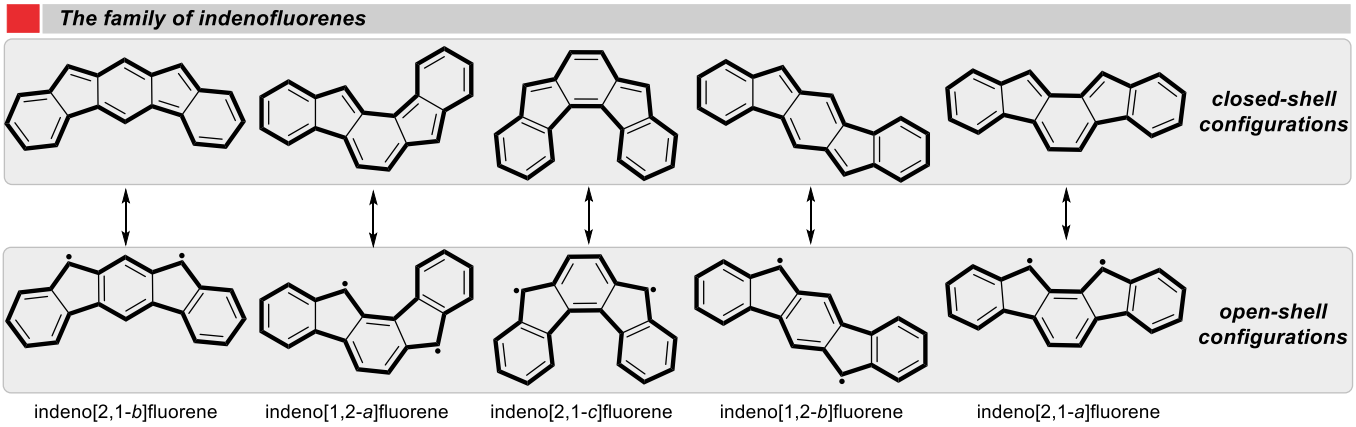

Figure 1. The five regioisomeric indenofluorenes

Herein we report the synthesis of the dibenzoindeno[2,1-c]fluorene **IF7H** (Figure 2, right), a [7]helicenoid with partial diradical character, and the study of its optoelectronic, magnetic and chiroptical properties. All the experimental data are supported by DFT-theoretical calculations.

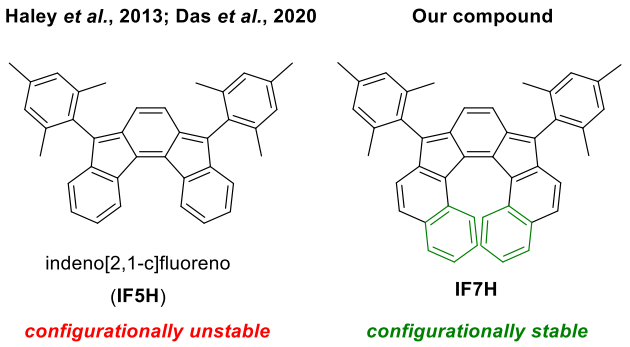

Figure 2. The simple indeno[2,1-*c*]fluorene **IF5H** (left) and our synthesized extended compound **IF7H** (right).

We carried out the synthesis of **IF7H** starting from the diketone **1**. For the synthesis of **1**, we followed the seven-steps synthesis described by Cadart *et al.* based on an enantioselective [2+2+2] cyclotrimerization of triynes and subsequent oxidation.[31] The diketone was obtained in a 60:40 *e.r.* (*P*:*M* ratio) as reported in literature. Then we carried out a nucleophilic addition reaction using 2,4,6-trimethylphenylmagnesium bromide to give diol **2** (Scheme 1). A final dearomatization reaction using $SnCl_2$ gave **IF7H** as a red solid, soluble in toluene or DCM among other organic solvents.

Scheme 1. Synthesis of dibenzoindeno[2,1-*c*]fluorene **IF7H**. Conditions: i) 2,4,6-trimethylphenylmagnesium bromide, THF, 0 °C; ii) $SnCl_2$, toluene, 40 °C. See SI for further details.

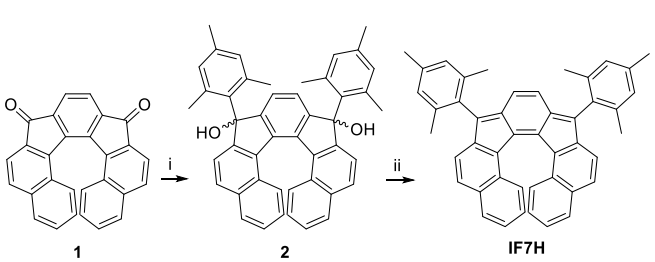

Compound **IF7H** showed a clear ^{1}H-NMR spectra with signals between 7.6 and 5.7 ppm in the aromatic region (Figure 3a) that slightly broaden at high temperature (378 K in 1,1,2,2-tetrachloroethane-d_2), featuring the thermal accessibility of the triplet state. High resolution electrospray ionization mass spectrometry analysis of **IF7H** showed a peak at m/z = 588.2822, in agreement with the theoretical molecular mass ($[M]^+$ = 588.2817). Also, its isotopic distribution pattern matched the theoretical one (See SI).

We obtained single crystals of moderate quality of compound **IF7H**, allowing its characterization by X-ray diffraction (Figure 3b-e). Alternating bond lengths of the central *as*-indacene unit agree with those previously reported for indeno[2,1-*c*]fluorene **IF5H**[4] confirming its closed-shell nature (Figure 3c). The degree of twisting was analyzed with the sum of the five helicene dihedral angles, resulting in a torsion of 64.4°-66.0° (Figure 3d), which is greater than the observed for dinor[7]helicene recently described.[24] However, this twisting is not uniformly distributed among all the dihedral angles. Those centered on the pentagonal rings are bigger than those centered on the hexagonal rings, with the former ranging between 23.8° and 31.5° (mean value 26.8°) and the latter being not larger than 6.0° (mean value: 3.9°) (Figure 3d).This is clearly a different feature from the one observed in [5]- or [7]helicenes, which show more homogeneous dihedral angles, ranging 17°-32°. Dinor[7]helicene also exhibit a different trend, as the bigger dihedral angle would be the one around the central benzene ring (corresponding to φ_3 in our case, Figure 3d), with a value of ca. 31°-33°, while those centered on the pentagonal rings are smaller (*ca.* 4°-6°). The interplanar angle between the mean planes of the outer benzene rings was 45.6°-46.3°, a similar value than that of [5]helicene (46°),[32] slightly smaller than the interplanar angle exhibited by the dinor[7]helicene (48.6°-51.1°) but larger than the corresponding value in the [7]helicene (32.0°). The distance between the centroids in those two rings was *ca.* 4.6 Å (Figure 3e), larger than that observed in [7]helicene (3.8 Å)[33] or the dinor[7]helicene (4.2-4.3 Å) and close to that of the [5]helicene (5.0 Å).

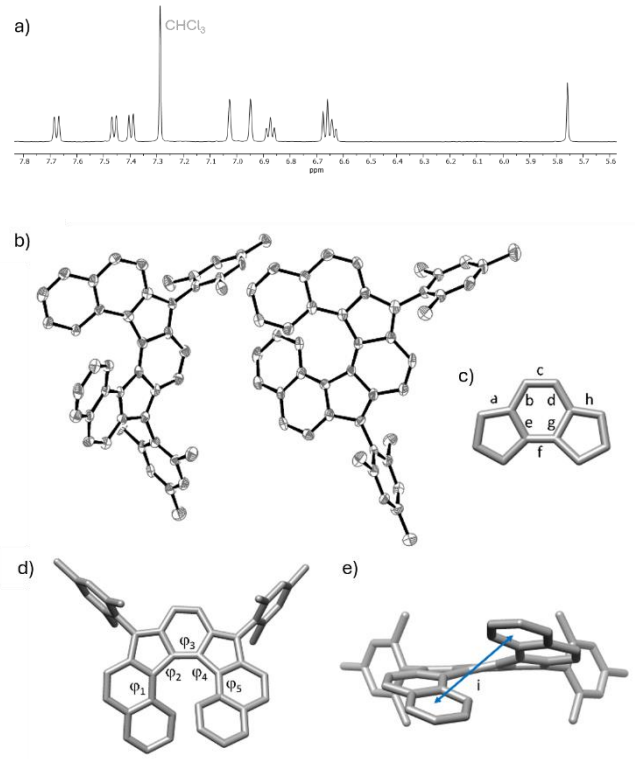

Figure 3. ^{1}H-NMR spectrum and single-crystal X-ray diffraction structure of compound **IF7H**. (a) Aromatic region of the ^{1}H-NMR spectrum (b) ORTEP drawing of the two molecules of **IF7H** present in the asymmetric unit. The thermal ellipsoids are shown at 50% probability. (c) Bond distances (in Å) in the *as*-indacene core: a, 1.37-1.38; b, 1.43; c, 1.35-1.36; d, 1.43; e, 1.48; f, 1.36-1.38, g, 1.49, h, 1.37; (d) Top view of the structure showing the dihedral angles (in °) in the helicene moiety: φ_1, 1.6-6.0; φ_2, 23.8-31.5; φ_3, 4.6-5.6; φ_4, 24.3-27.4; φ_5, 2.5-3.1; (e) front view showing the distance between the outer helicene rings: i, 4.61-4.63 Å. H atoms have been omitted for clarity in all structures. Two values are given for some distances and angles as there are two molecules of **IF7H** in the asymmetric unit.

Then we investigated its photophysical properties (Figure 4a). Compound **IF7H** presented an absorption profile spanning from 250 nm to 550 nm. The lowest energy band covered the range 450-550 nm (λ_{max} = 517 nm, $\varepsilon = 0.60 \times 10^4$ M^{-1} cm^{-1}). This band is red-shifted compared to the one in **IF5H**. Time-dependent DFT (TDDFT) calculations were carried out at the B3LYP/6-311G(d) level of theory. The calculated transitions for **IF7H** matched the experimental UV-vis, we found a transition at 520.63 nm (f = 0.224) with a 90% HOMO-1→LUMO character. The lowest energy transition appeared at 956.89 nm (f = 0.0146) and is described with a pure HOMO→LUMO character. However, we could not experimentally identify it, due to its low oscillator strength and its broadness. As for other IF derivatives, compound **IF7H** is non-emissive.[34]

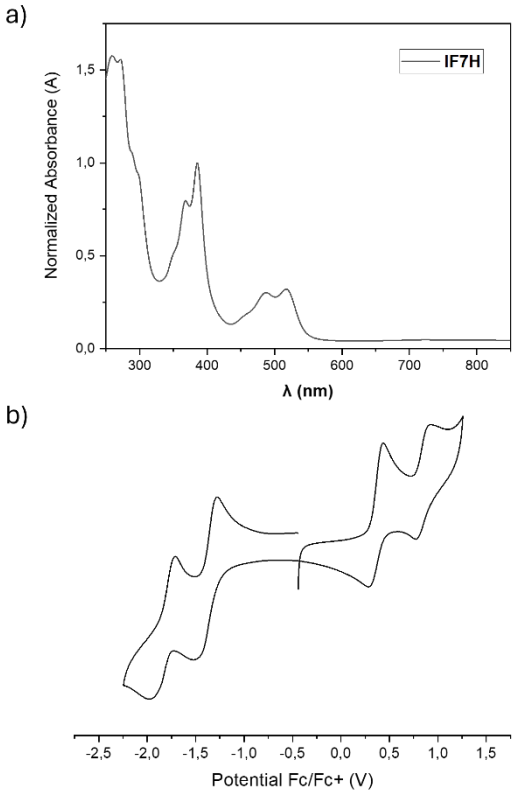

Figure 4. (a) UV-Vis of **IF7H**; (b) voltammogram of **IF7H**.

Then, we carried out cyclic voltammetry (CV) to inspect the electrochemical behavior of **IF7H** (Figure 4b). Compound **IF7H** showed ambipolar character, presenting two reversible oxidation peaks at +0.37 V and +0.85 V, and two reversible reduction peaks at –1.38 V and –1.85 V. The HOMO energy was estimated in –5.17 eV, ~0.5 eV higher than the reported for **IF5H**.[4] The LUMO energy was –3.42 eV. Consequently, the electrochemical HOMO-LUMO gap was estimated to be 1.73 eV, ~0.3 eV lower than for **IF5H**. Theoretical calculations agreed with the experimental results, estimating a HOMO-LUMO gap of 1.94 eV.

Next, we investigated its magnetic properties. As mentioned, the ^{1}H NMR spectrum of **IF7H** showed well-resolved signals even at high temperatures. However, this compound is active to electron paramagnetic resonance (EPR) (see SI, section 8). We observed a featureless and weak peak at room temperature centered at g = 2.0025 although we did not observe any half-field signal corresponding to $\Delta m = \pm 2$ transition featuring the triplet state. We also investigated its magnetic susceptibility with a superconducting quantum interference device (SQUID) magnetometer. The measurements for the powder sample of **IF7H** show a very low and constant value of the $\chi_m T$ product (χ_m is the molar magnetic susceptibility) between 50-300 K and a pronounced increase from 300 K because of thermal population of the S = 1 spin state (Figure 5a). From the Bleaney-Blowers fitting, the singlet-triplet energy gap (ΔE_{S-T}) was determined to be 9.36 kcal mol^{-1} which agrees with the computed value (8.32 kcal mol^{-1}). The calculated singlet-triplet gap for **IF5H** was 13.34 kcal mol^{-1} indicating that the extension of the structure, that promotes a more pronounced distortion, lower the gap considerably.

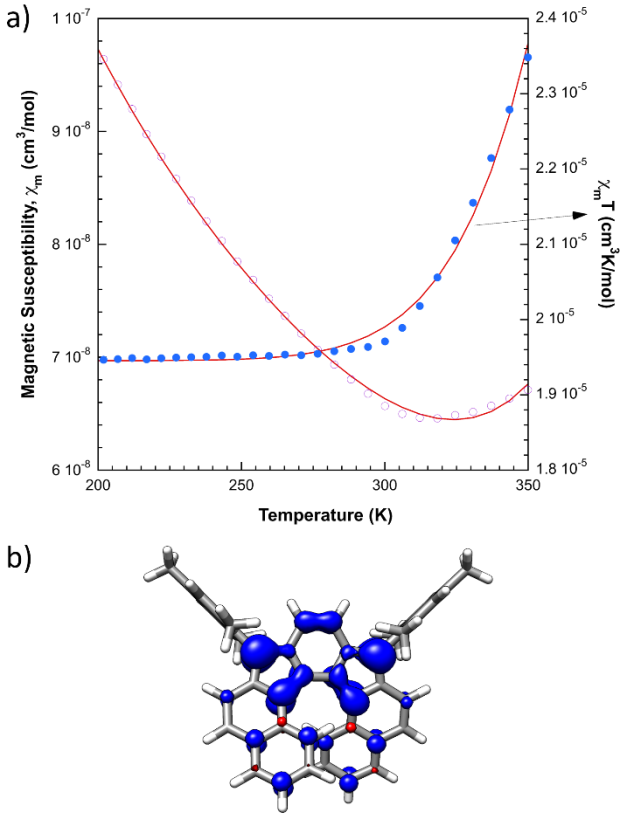

Figure 5. (a) SQUID measurement for **IF7H**; (b) spin density distribution in calculated by DFT (UB3LYP/6-311G(d)).

We carried out further theoretical calculations to rationalize the magnetic behavior of our structure. Diradical index y_0 is a theoretical parameter that gives an idea of the contribution of the open-shell configuration to the overall structure.[35] We carried out the calculations using complete active space self-consistent field (CASSCF(12,12)) and they indicate a mainly closed-shell configuration for **IF7H** (y_0 = 0.07), in accordance with the experimental results. To gain more insight in the spin local distribution we calculated the spin density for **IF7H** using DFT and UB3LYP/6-311G(d) basis. As shown in Figure 5b, the compound presents spin density mainly around the apical five-membered rings carbon atoms, the central phenyl ring and the inner part of the helicene. Additionally, some spin density locates in the outer ring.

Finally, we attempted the isolation of the enantiomers and the investigation of their chiroptical properties. Unfortunately, **IF7H** was not separable by chiral HPLC in any tested conditions. As enantiomers of diketone **1** (60:40 *e.r.*) were also not possible to fully separate by chiral HPLC, we focus on compound **2**. Diastereoisomers were separated by flash column chromatography and further purified by chiral HPLC. Assignation of the *R*/*S* stereocenters were not carried out as it is inconsequential for the outcome of the final reaction. Finally, after dearomatization using $SnCl_2$ the two enantiomers *P*-**IF7H** and *M*-**IF7H** were obtained (See SI). As shown in Figure 6, the enantiopure samples displayed mirror-images electronic circular dichroism spectra (ECD) with g_{abs} values up to 1.2×10^{-3} (λ = 308 nm). The absolute configuration of each enantiomer was assigned by TD-DFT. Additionally, configurational stability was studied calculating $\Delta G^{\ddagger}_{rac}$ value. We followed experimentally the decay of the ECD signal with the temperature for a given enantiomer. We calculated a $\Delta G^{\ddagger}_{rac}$ of 24.64 kcal mol^{-1} at 298 K. The racemization rate constant, *k*, allows to estimate a racemization half-life, ($t_{1/2}$) of 3.6 days at 298 K.

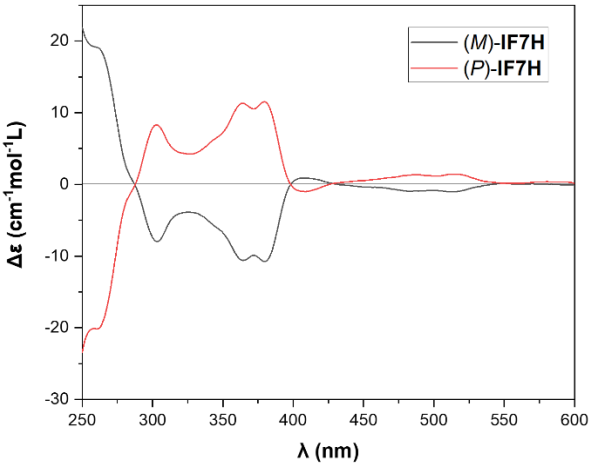

Figure 6. ECD spectra of **IF7H**.

In conclusion, we have synthesized the simplest configurationally stable helically chiral indenofluorene and evaluated their optoelectronic, magnetic and chiroptical properties. **IF7H** showed absorption up to 550 nm, a low HOMO-LUMO gap (1.73 eV) and ambipolar character. The molecule presented a mainly closed-shell structure with a diradical character index of 0.07 and a singlet-triplet gap of 9.36 kcal mol^{-1}. The configurationally stability of **IF7H** ($\Delta G^{\ddagger}_{rac}$ = 24.64 kcal mol^{-1} at 298 K) led the measurement of ECD for each enantiomer. The dissymmetry factor (g_{abs}) reached 1.2×10^{-3}. These features, together with its chemical robustness, made this chiral molecule with partial diradical character suitable for optoelectronic and chirospintronic application.

ASSOCIATED CONTENT

Supporting Information

The Supporting Information is available free of charge on the ACS Publications website.
Experimental and computational details, synthesis and characterization of compounds, copies of NMR spectra, high resolution mass spectrum, RX details, EPR spectrum, chiral separation details and chromatograms (PDF)

Accession Codes
CCDC 2323643 contains the supplementary crystallographic data for this paper. These data can be obtained free of charge via www.ccdc.cam.ac.uk/data_request/cif, or by emailing da-ta_request@ccdc.cam.ac.uk, or by contacting The Cambridge Crystallographic Data Centre, 12 Union Road, Cambridge CB2 1EZ, UK; fax: + 44 1223 336033.

AUTHOR INFORMATION

Corresponding Author

* Carlos M. Cruz – *Departamento de Química Orgánica y Unidad de Excelencia de Química aplicada a Biomedicina y Medioambiente, Facultad de Ciencias, Universidad de Granada, 18071 Granada, Spain;* Email: cmorenoc@ugr.es

* Alba Millán – *Departamento de Química Orgánica y Unidad de Excelencia de Química aplicada a Biomedicina y Medioambiente, Facultad de Ciencias, Universidad de Granada, 18071 Granada, Spain*; Email: amillan@ugr.es

Author Contributions

All authors have given approval to the final version of the manuscript.

Notes

The authors declare no competing financial interest.

ACKNOWLEDGMENT

This work received financial support from grant PID2021-127964NB-C22 funded by MICIU/AEI/ 10.13039/501100011033 and ERDF, EU. C.M.C. thanks Junta de Andalucía for a postdoctoral grant (POSTDOC_21_00139) and the financial support from grant PID2022-137403NA-I00 funded by MICIU/AEI/ 10.13039/501100011033 and ERDF, EU. A.M.-P. thanks Ministerio de Universidades for a FPU contract (FPU19/03751). R. C. acknowledges grant PRE2018-083406 funded by MICIU/AEI/ 10.13039/501100011033 and by "ESF Investing in your future". We thank Centro de Servicio de Informática y Redes de Comunicaciones (CSIRC), Universidad de Granada, for providing the computing time.
n.

REFERENCES

(1) Can, A.; Facchetti, A.; Usta, H. Indenofluorenes for Organic Optoelectronics: the Dance of Fused Five- and Six-Membered Rings Enabling Structural Versatility. *J. Mater. Chem. C*, **2022**, *10*, 8496–8535.

(2) Shimizu, A.; Kishi, R.; Nakano, M.; Shiomi, D.; Sato, K.; Takui, T.; Hisaki, I.; Miyata, M.; Tobe, Y. Indeno[2,1-*b*]fluorene: A 20-π-Electron Hydrocarbon with Very Low-Energy Light Absorption. *Angew. Chem., Int. Ed.* **2013**, *52*, 6076–6079.

(3) Dressler, J. J.; Zhou, Z.; Marshall, J. L.; Kishi, R.; Takamuku, S.; Wei, Z.; Spisak, S. N.; Nakano, M.; Petrukhina, M. A.; Haley M. M. Synthesis of the Unknown Indeno[1,2-*a*]fluorene Regioisomer: Crystallographic Characterization of Its Dianion. *Angew. Chem., Int. Ed.* **2017**, *56*, 15363–15367.

(4) Fix, A. G.; Deal, P. E.; Vonnegut, C. L.; Rose, B. D.; Zakharov, L. N.; Haley, M. M. Indeno[2,1-*c*]fluorene: A New Electron-Accepting Scaffold for Organic Electronics. *Org. Lett.* **2013**, *15*, 1362–1365.

(5) Sharma, H.; Ankita, A.; Bhardwaj, P.; Pandey, U. K.; Das, S. Exploring Indeno[2,1-*c*]fluorene Antiaromatics with Unsymmetrical Disubstitution and Balanced Ambipolar Charge-Transport Properties. *Organic Materials* **2023**, *5*, 72–83.

(6) Chase, D. T.; Fix, A. G.; Rose, B. R.; Weber, C. D.; Nobusue, S.; Stockwell, C. E.; Zakharov, L. N.; Lonergan, M. C.; Haley, M. M. Electron-Accepting 6,12-Diethynylindeno[1,2-*b*]fluorenes: Synthesis, Crystal Structures, and Photophysical Properties. *Angew. Chem., Int. Ed.* **2011**, *50*, 11103–11106.

(7) Chase, D. T.; Rose, B. D.; McClintock, S. P.; Zakharov, L. N.; Haley, M. M. Indeno[1,2-*b*]fluorenes: Fully Conjugated Antiaromatic Analogues of Acenes. *Angew. Chem., Int. Ed.* **2011**, *50*, 1127–1130.

(8) Chase, D. T.; Fix, A. G.; Rose, B. R.; Weber, C. D.; Nobusue, S.; Stockwell, C. E.; Zakharov, L. N.; Lonergan, M. C.; Haley, M. M. Electron-Accepting 6,12-Diethynylindeno[1,2-*b*]fluorenes: Synthesis, Crystal Structures, and Photophysical Properties. *Angew. Chem., Int. Ed.* **2011**, *50*, 11103–11106.

(9) Chase, D. T; Fix, A. G.; Kang, S. J.; Rose, B. D.; Weber, C. D.; Zhong, Y.; Zakharov, L. N.; Lonergan, M. C.; Nuckolls, C.; Haley, M. M. 6,12-Diarylindeno[1,2-*b*]fluorenes: Syntheses, Photophysics, and Ambipolar OFETs. *J. Am. Chem. Soc.* **2012**, *134*, 10349–10352.

(10) Nishida, J.-i.; Tsukaguchi, S.; Yamashita, Y. Synthesis, Crystal Structures, and Properties of 6,12-Diaryl-Substituted Indeno[1,2-*b*]fluorenes. *Chem. Eur. J.* **2012**, *18*, 8964–8970.

(11) Casares, R.; Martínez-Pinel, Á.; Rodríguez-González, S.; Márquez, I. R.; Lezama, L.; González, M. T.; Leary, E.; Blanco, V.; Fallaque, J. G.; Díaz, C.; Martín, F.; Cuerva, J. M.; Millán, A. Engineering the HOMO–LUMO Gap of Indeno[1,2-*b*]fluorene. *J. Mater. Chem. C* **2022**, *10*, 11775–11782.

(12) Sharma, H.; Bhardwaj, N.; Das, S. Revisiting Indeno[1,2-*b*]fluorene by Steric Promoted Synthesis while Isolating the Second Stable 4nπ Indeno[2,1-*a*]fluorene. *Org. Biomol. Chem.* **2022**, *20*, 8071–8077.

(13) Shimizu, A.; Tobe, Y. Indeno[2,1-a]fluorene: An Air-Stable ortho-Quinodimethane Derivative. *Angew. Chem., Int. Ed.* **2011**, *50*, 6906–6910.

(14) Kubo, T. Recent Progress in Quinoidal Singlet Biradical Molecules. *Chem. Lett.* **2015**, *44*, 111–122.

(15) Casado, J. Para-Quinodimethanes: A Unified Review of the Quinoidal-Versus-Aromatic Competition and its Implications. *Top. Curr. Chem.* **2017**, *375*, 73.

(16) Kato, K.; Osuka, A. Platforms for Stable Carbon-Centered Radicals. *Angew. Chem., Int. Ed.* **2019**, *58*, 8978–8986.

(17) Tang, B.; Zhao, J.; Xu, J.-F.; Zhang, X. Tuning the Stability of Organic Radicals: from Covalent Approaches to Non-Covalent Approaches. *Chem. Sci.* **2020**, *11*, 1192–1204.

(18) Tani, F.; Narita, M.; Murafuji, T. Helicene Radicals: Molecules Bearing a Combination of Helical Chirality and Unpaired Electron Spin. *ChemPlusChem* **2020**, *85*, 2093–2104.

(19) Li, Q.; Zhang, Y.; Xie, Z.; Zhen, Y.; Hu, W.; Dong, H. Polycyclic Aromatic Hydrocarbon-Based Organic Semiconductors: Ring-closing Synthesis and Optoelectronic properties. *J. Mater. Chem. C* **2022**,*10*, 2411–2430.

(20) Mondal, P. C.; Mtangi, W.; Fontanesi, C. Chiro-Spintronics: Spin-Dependent Electrochemistry and Water Splitting Using Chiral Molecular Films. *Small Methods* **2018**, *2*, 1700313.

(21) Evers, F.; Aharony, A.; Bar-Gill, N.; Entin-Wohlman, O.; Hedegård, P.; Hod, O.; Jelínek, P.; Kamieniarz, G.; Lemeshko, M.; Michaeli, K.; Mujica, V.; Naaman, R.; Paltiel, Y.; Refaely-Abramson, S.; Tal, O.; Thijssen, J.; Thoss, M.; van Ruitenbeek, J. M.; Venkataraman, L.; Waldeck, D. H.; Yan, B.; Kronik, L. Theory of Chirality Induced Spin Selectivity: Progress and Challenges. *Adv. Mater.* **2022**, *34*, 2106629.

(22) Gao, M.; Qin, W. Organic Chiral Spin-Optics: The Interaction between Spin and Photon in Organic Chiral Materials. *Adv. Opt. Mater.* **2021**, *9*, 2101201.

(23) Hsieh, Y.-C.; Wu, C.-F.; Chen, Y.-T.; Fang, C.-T.; Wang, C.-S.; Li, C.-H.; Chen, L.-Y.; Cheng, M.-J.; Chueh, C.-C.; Chou, P.-T.; Wu, Y.-T. 5,14-Diaryldiindeno[2,1-*f*:1′,2′-*j*]picene: A New Stable [7]Helicene with a Partial Biradical Character. *J. Am. Chem. Soc.* **2018**, *140*, 14357–14366.

(24) Borissov, A.; Chmielewski, P. J.; Gómez García, C. J.; Lis, T.; Stępień, M. Dinor[7]helicene and Beyond: Divergent Synthesis of Chiral Diradicaloids with Variable Open-Shell Character. *Angew. Chem., Int. Ed.* **2023**, *62*, e202309238.

(25) Ma, J.; Liu, J.; Baumgarten, M.; Fu, Y.; Tan, Y.-Z.; Schellhammer, K. S.; Ortmann, F.; Cuniberti, G.; Komber, H.; Berger, R.; Müllen, K.; Feng, X. A Stable Saddle-Shaped Polycyclic Hydrocarbon with an Open-Shell Singlet Ground State. *Angew. Chem., Int. Ed.* **2017**, *56*, 3280–3284.

(26) Jiang, Q.; Han, Y.; Zou, Y.; Phan, H.; Yuan, L.; Herng, T. S.; Ding, J.; Chi, C. S-shaped para-Quinodimethane-Embedded Double [6]Helicene and Its Charged Species Showing Open-Shell Diradical Character. *Chem. Eur. J.* **2020**, *26*, 15613–15622.

(27) Frederickson, C. K.; Lev N. Zakharov, L. N.; Haley, M. M. Modulating Paratropicity Strength in Diareno-Fused Antiaromatics. *J. Am. Chem. Soc.* **2016**, *138*, 16827–16838.

(28) Ortiz, R. P.; Casado, J.; Hernández, V.; López Navarrete, J. T.; Viruela, P. M.; Ortí, E.; Takimiya, K.; Otsubo, T. On the Biradicaloid Nature of Long Quinoidal Oligothiophenes: Experimental Evidence Guided by Theoretical Studies. *Angew. Chem., Int. Ed.* **2007**, *46*, 9057–9061.

(29) Ravat, P.; Šolomek, T.; Rickhaus, M.; Häussinger, D.; Neuburger, M.; Baumgarten, M.; Juríček, M. Cethrene: A Helically Chiral Biradicaloid Isomer of Heptazethrene. *Angew. Chem., Int. Ed.* **2016**, *55*, 1183–1186.

(30) Ravat, P.; Šolomek, T.; Ribar, P.; Juríček, M. Biradicaloid with a Twist: Lowering the Singlet–Triplet Gap. *Synlett* **2016**, *27*, 1613–1617.

(31) Cadart, T.; Nečas, D.; Kaiser, R. P.; Favereau, L.; Císařová, I.; Gyepes, R.; Hodačová, J.; Kalíková, K.; Bednárová, L.; Crassous, J.; Kotora, M. Rhodium-Catalyzed Enantioselective Synthesis of Highly Fluorescent and CPL-Active Dispiroindeno[2,1-*c*]fluorenes. *Chem. Eur. J.* **2021**, *27*, 11279–11284.

(32) Kuroda, R. J. Crystal and Molecular Structure of [5]helicene: Crystal Packing Modes. *J. Chem. Soc. Perkin Trans. 2* **1982**, 789 –794.

(33) Fuchter, M. J.; Weimar, M.; Yang, X.; Judge, D. K.; White, A. J. P. An Unusual Oxidative Rearrangement of [7]-helicene. *Tetrahedron Lett.* **2012**, *53*, 1108–1111.

(34) Rose, B. D.; Shoer, L. E.; Wasielewski, M. R.; Haley, M. M. Unusually Short Excited State Lifetimes of Indenofluorene and Fluorenofluorene Derivatives Result from a Conical Intersection. *Chem. Phys. Lett.* **2014**, *616-617*, 137–141.

(35) Nakano, M. *Top. Curr. Chem.* **2017**, *375*, 47.